17th World Conference on Earthquake Engineering, 17WCEE
Sendai, Japan - September 13th to 18th 2020

PERFORMANCE-BASED PLASTIC DESIGNED FOR BUCKLING-RESTRAINED BRACED FRAMES

R. M. Oinam[(1)], M. K. Nadimpally [(2)], P. V. Kunaparaju[(3)]

[(1)]*Assistant Professor, Indian Institute of Technology Tirupati, romanbabu@iittp.ac.in*
[(2)] *Undergraduate Student, Indian Institute of Technology Tirupati, ce17b017@iittp.ac.in*
[(3)] *Undergraduate Student, Indian Institute of Technology Tirupati, ce17b013@iittp.ac.in*

Abstract

Buckling Restrained Brace (BRB) is one of the most effective passive energy dissipation devices which is applicable in both seismic rehabilitation and new construction. In this study, the steel frames are designed as a moment frame and dual system frames using Performance-Based Plastic Design (PBPD). In the dual system frame, BRBs are used as passive energy dissipation devices, which have been configured in two different orientations. These study frames have been modeled in the *OpenSees* platform, and non-linear static pushover and non-linear time history analysis have been carried out. Seven sets of ground motion are used for non-linear dynamic analysis, which is compatible with the seismic hazard level of design basis earthquake (DBE) as per Indian seismic code. The fiber section has been used extensively throughout the model to consider the inelastic deformation on the frame members. Various parameters are investigated in this study like failure mechanism, energy dissipation capacity, ductility, and lateral load distribution in the Buckling Restrained Braced Frame (BRBF) systems. A comparative study for each parameter of all study frames is reported.

Keywords: Steel moment-resisting frame; Dual system; Buckling restrained braces; Yield mechanism; Earthquake.

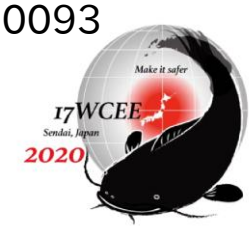

1. Introduction

Buckling Restrained Brace (BRB) is one of the most effective passive energy dissipation devices which is applicable in both seismic rehabilitation and new construction. This device is an updated version of a conventional brace member by restricting buckling under axial load. The specialty of BRBs is yielding in both tension and compression. As a result, it has symmetric hysteresis response under the cyclic loading (like wind and earthquake). With the absence of premature instability, it has high performance in terms of ductility, energy dissipation capacity, and a smaller amount of cumulative deformation [1]. These characteristics could be utilized in Buckling Restrained Braced Frame (BRBF) systems to improve energy dissipation capability, strength, and stiffness as well as control of the inter-story drift response. However, in the BRBF systems, a significant residual displacement is accompanied due to low postyield stiffness of BRBs when subjected to moderate-to-high level seismic excitations. Especially in ductile structure, complete demolition in post-earthquake is quite common due to excess residual inter-story drift, which reflects the economy of the society. Some previous studies suggest that if the inter-story drift ratios are greater than 0.5%, the building is no longer practically usable [2]. On the other side, recent analytical studies show that the allowable average peak residual drift ratios for the BRBF systems can vary from 0.8 to 2.0% under the Design Basis Earthquake (DBE) [2]. Besides, if the residual drift is high, the structure might completely collapse under the aftershocks. In this study, considering all these issues, a three-story building is designed as moment frame and dual system frames using Performance-Based Plastic Design method (PBPD), which is superior over the displacement and co-efficient based design method *(i.e., response reduction factor "R" method)* [4]. In the dual system frame, BRBs are used as passive energy dissipation devices. Two types of dual system frame are considered here to check the effectiveness of BRBs. Details of these study frames are extensively discussed in the following sections.

2. Performance-based plastic design (PBPD)

Performance-Based Plastic Design (PBPD) is energy balanced design approach that was introduced by Housner (1956) [6]. Fig. 1a shows the underlying philosophy of the PBPD design method, along with a preferable yield mechanism. In this design method, total seismic input energy has calculated by pushing the structure monotonically up to a maximum target deformation. The seismic input energy is the function of structural ductility factor (μ_s) and ductility reduction factor (R_μ). These parameters could be calculated using the plot shown in Fig. 1 (b, c). This design method is adopted in this study to design a moment frame as well as a dual system frame. In PBPD, predefined yield drift, target drift, and yield mechanism are the key performance states. These parameters could be chosen based on experimental literature and the concept of a strong column weak beam. Details are provided in the design section.

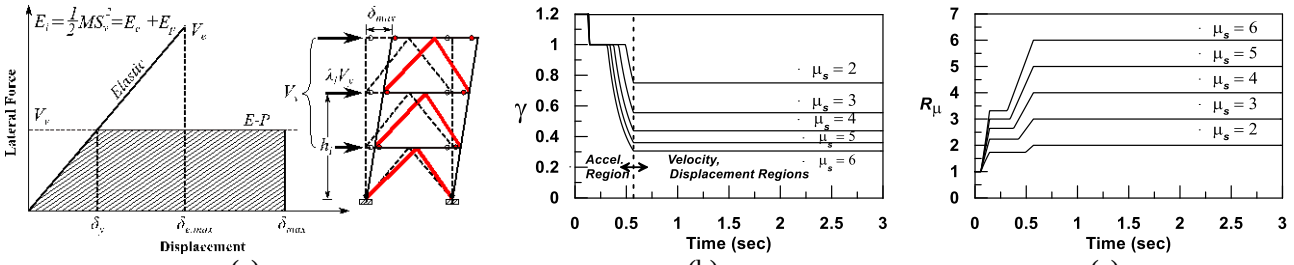

(a) (b) (c)

Fig. 1 – Philosophy of performance-based plastic design (a) Energy balance concept with yield mechanism (b) Energy modification factor and (c) Idealized inelastic spectra

As per this design method, yield base shear (V_y) can be calculated from the given equation:

$$\frac{V_y}{W} = \frac{-\alpha + \sqrt{\alpha^2 + 4\left(\gamma/\eta\right)S_a^{\,2}}}{2} \qquad (1)$$

Where W is seismic weigh, S_a is normalized pseudo-acceleration and η is a modification factor to consider pinching behavior. For the BRB system η is recommended as 0.9 [6]. Furthermore, α is a dimensionless parameter. The value of α depends on the stiffness, modal properties, and plastic drift level of the structural system as follows:

$$\alpha = \frac{8\pi^2 \theta_p h_l}{T^2 g} \cong \frac{8\theta_p h_l}{T^2} \tag{2}$$

Where, θ_p is inelastic drift, h_l is equivalent story height, g is the acceleration due to gravity, and T is the fundamental period.

3. Study frame

A three-story building has been used for the design and evaluation of seismic performance. The site location of this building is soil type A, which has seismic zone factor V (*i.e., Z=0.36*) as per IS: 1893-I [7]. The typical bay width of the building is 5.0 m, and the height of the floor is 4.0 m for each story. The seismic weight of the building is 28910 kN. The frames were designed as a moment frame as well as a dual system. In the dual system, BRBs have been configured in two ways (a) diagonal braces in the outer bay (i.e., BRBF-I) and (b) diagonal braces in inner bays (i.e., BRBF-II). Details of the study frames, along with the plan, are shown in Fig. 2.

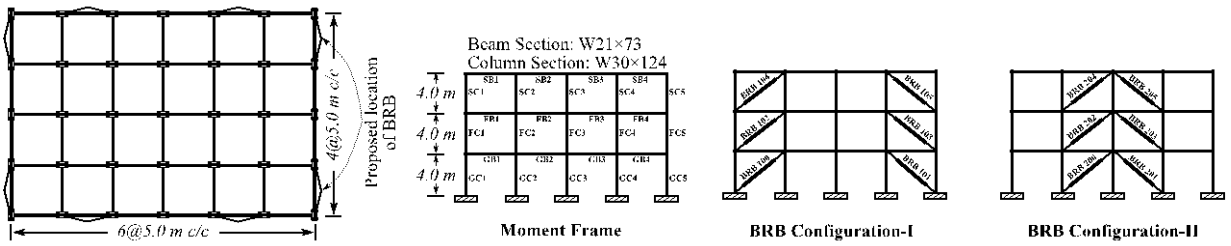

(a) (b) (c) (d)

Fig. 2 – Details of the study frame (a) plan, (b) moment-resisting frame, (c, d) different BRB configuration in dual system

3.1. Design of frame members

A predefined yield mechanism (Fig.1a) has been assumed for the design of structural members. As per this mechanism, yielding is going to occur only at the base of the ground columns and BRB. A target drift (θ_u) and yield drift (θ_y) have been taken as 4.0% and 0.3%, respectively. Here, target and yield drifts are defined based on experimental literature, while yield mechanism is chosen based on desirable yielding pattern considering strong column weak beam concept. As per demand on the members, section capacities have been designed using nominal material strengths. Table 1 shows the material characteristics of the members. A typical schematic view of BRB is shown in Fig. 3, and the force *vs.* deformation backbone of BRBs is shown in Table 2.

Table 1 – Structural steel section properties

Yield		**Ultimate**		**Fracture**		**Modulus of Elasticity**	**Poison ratio**
Stress (MPa)	Strain	Stress (MPa)	Strain	Stress (MPa)	Strain	*E (MPa)*	*v*
250	0.0013	280	0.0023	300	0.0043	$2*10^5$	0.3

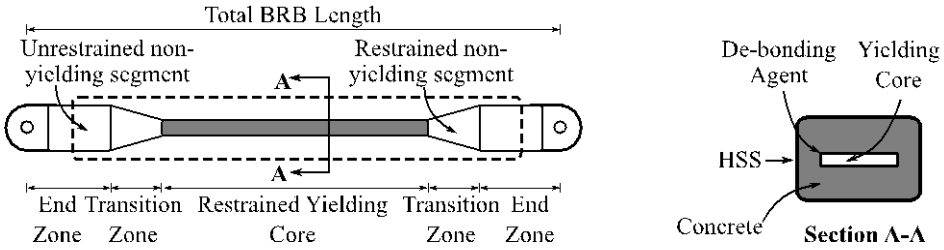

Fig. 3 –Schematic diagram of BRB longitudinal and cross-sectional details

Table 2 – Force deformation characteristics of BRBs

Yield		Ultimate		Fracture	
Force (kN)	Deform. (mm)	Force (kN)	Deform. (mm)	Force (kN)	Deform. (mm)
300	5	350	20	400	42

4. Numerical modeling

OpenSees platform is used to model and simulate the seismic response of structural systems. Inelastic deformation of structural members has been considered in the model using the fiber section, which has the capability of capturing axial deformation as well as flexural deformation. Since the metal structure did not show any shear dominant failure pattern, shear deformation is not included in the model. Fig. 4a shows the modeling of structural members using nonlinear displacement-based fiber-type beam-column elements, and Fig. 4b shows the mechanics of the fiber section. Five integration points have been used in the potential plastic hinge region to capture the realistic failure mode. Based on the position of fiber grid, stress-strain characteristics and geometric properties of fiber sections, the axial capacity *(P)*, flexural strength *(M_z)*, and their interaction on the load-carrying capacity of a frame member are incorporated in the numerical model.

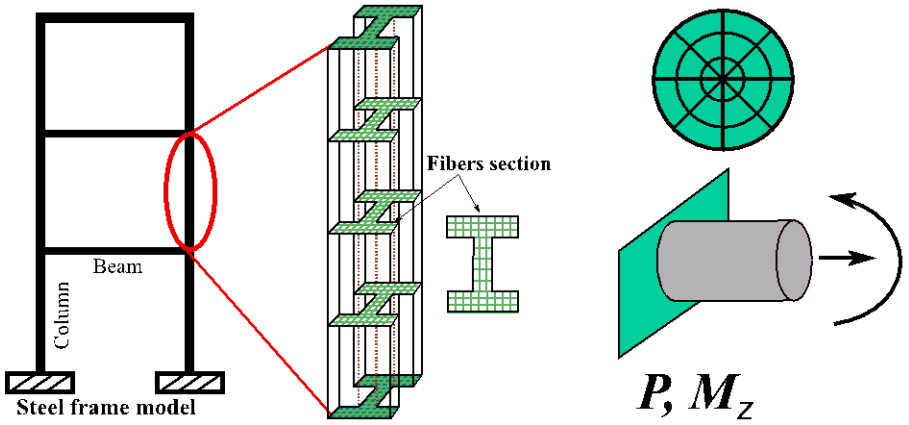

(a) (b)

Fig. 4 – Details of section modeling (a) fiber section assigned in members and (b) mechanism of fiber section

While modeling beam and column, a uniaxial material called "*Hysteretic material*" has been used. The nonlinear monotonic behavior of Steel material is characterized by a multi-linear curve defined by eleven parameters as shown in Fig. 5. These parameters are (i) compression yield strain and stress coordinate *(e_{1p}, s_{1p})*; (ii) compression intermediate strain and stress coordinate *(e_{2p}, s_{2p})*; (iii) compression ultimate strain and stress coordinate *(e_{3p}, s_{3p})*; (iv) tension yield strain and stress coordinate *(e_{1n}, s_{1n})*; (v) tension intermediate strain and stress coordinate *(e_{2n}, s_{2n})*; (vi) tension ultimate strain and stress coordinate *(e_{3n}, s_{3n})*; (vii) pinching factor for strain during reloading (*$pinch_x$*); (viii) pinching factor for stress during reloading (*$pinch_y$*); (ix) damage due to ductility (*$damage_1$*); (x) damage due to energy (*$damage_2$*);

(xi) power used to determine the degraded unloading (*$beta*). Material behavior has been modeled symmetrically in tension and compression and corresponding stress-strain coordinate has been taken from Table 1. Furthermore, *$pinch$_x$*; *$pinch$_y$*; *$damage$_1$*; *$damage$_2$* and *$beta* have been taken as 0.8, 0.2, 0, 0 and 0 respectively for beams and columns.

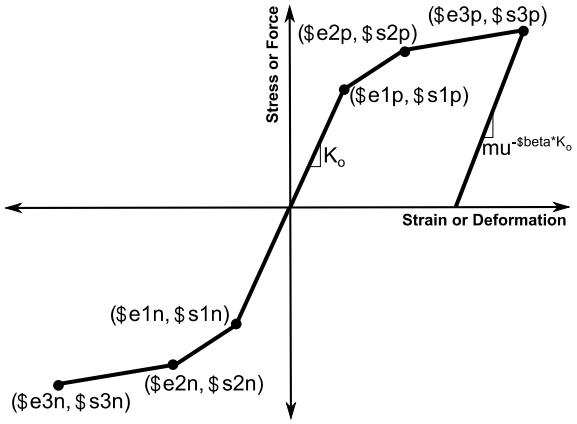

Fig. 5 – Response of Hysteretic material [8]

The same uniaxial material (i.e., *Hysteretic material*) has been used for BRB modeling. However, in this condition, the force-deformation values have been assigned instead of stress-strain data. The symmetrical force deformation data has been taken from Table 2. The data of other parameters like *$pinch$_x$*; *$pinch$_y$*; *$damage$_1$*; *$damage$_2$* and *$beta* have been taken as 1.0, 1.0, 0, 0 and 0.5 respectively.

5. Performance of study frames

Linear modal analysis was conducted to determine the fundamental periods of the study frames. The moment frame, BRBF configuration-I, and BRBF configuration-II frames exhibited the natural periods of 0.36, 0.26, and 0.25 sec respectively. Two non-linear analysis, namely (a) static pushover and (b) dynamic time-history analyses, have been carried out to check the effectiveness of BRBs under various loading conditions. For dynamics time-history analysis, seven recorded ground motions were selected, which is summarized in Table 3. Fig. 6 shows the acceleration time-history of selected ground motions and the comparison of the target response spectrum with a 5% damped response spectra of the ground motions. Target Design-Basis Earthquake (DBE) spectrum is obtained by dividing a factor of 1.5 to the Maximum Considered Earthquake (MCE) spectrum for the seismic zone-V, and hard soil as per Indian Standard IS:1893-I provisions [7].

Table 3 –Earthquake data and site information of selected ground motions

Name of Earthquake	Station	Comp.	Mag. (M_w)	Dist. (km)	PGA (g)	Soil	Mechanism
Chamoli, India (1999)[a]	Gopeshwar	20	6.6	17.3	0.36	Rock	Strike-slip
Chi-Chi, Taiwan (1999)[b]	Taichung	90	7.6	8.3	0.32	Soft	Reverse-oblique
Elcentro, CA (1940)[b]	Elcentro	180	6.9	12.2	0.35	Alluvium	Strike-slip
Hector Mine, CA (1999)[b]	Hector	180	7.13	11.7	0.27	Alluvium	Strike-slip
Imperial Valley, CA (1979)[b]	Delta	180	6.53	22.0	0.24	Alluvium	Strike-slip
Kobe, Japan (1995)[b]	Kakogawa	90	6.9	22.5	0.34	Soft	Strike-slip
Kocaeli, Turkey (1999)[b]	Arcelik	0	7.51	13.5	0.21	Alluvium	Strike-slip

[a]Strong Motion Centre (SMC); [b]Pacific Earthquake Engineering Research (PEER).

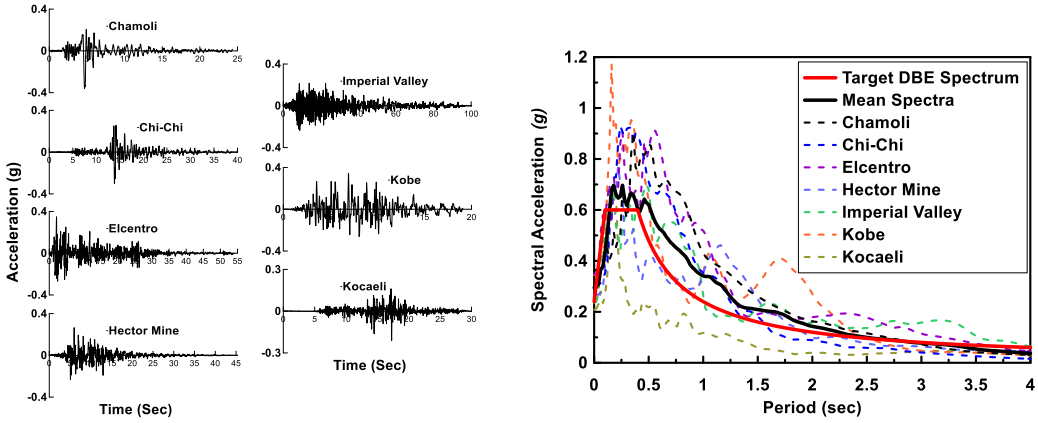

(a) (b)

Fig. 6 – Typical information of grond motions (a) acceleration-time histories and (b) comparing the mean response spectra of the selected ground motions with the target spectrum

5.1. Push-over

Nonlinear static pushover analysis was carried out on the study frames. Gradually increasing displacement-controlled loadings were applied to the study frames until a story drift of 4.0%. The lateral displacement profiles resembling the fundamental mode shapes of the study frame are applied during the analysis. Fig. 7 shows the comparison of lateral strength versus drift response and the hinge mechanism of the study frames. At a drift of 4%, the moment frame carried a maximum lateral load of 4204.3 kN, while BRB configuration-I & II carried maximum loads of 5857.6 kN and 5929.2 kN, respectively. Base shear vs. drift response of all three frames is shown in Fig. 7a. The yield mechanism of study frames under static push over drift is shown in Fig. 7b.

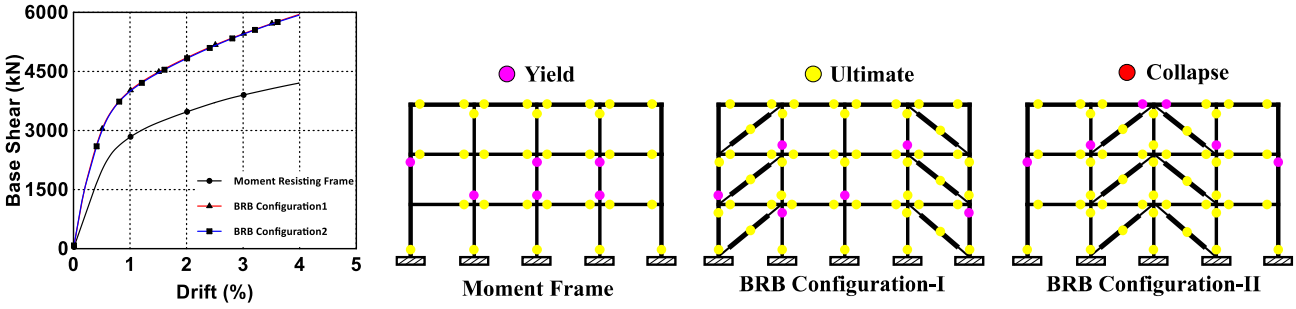

(a) (b)

Fig. 7 – Comparison of (a) pushover curves (b) hinge mechanisms of study frames at a drift level of 4.0%

In the moment frame, flexural yielding occurs in all ground, first-floor, and top floor beams. The deformation level of these beams is near to ultimate. Also, all ground column reaches the ultimate flexural strength. However, these members did not reach their collapse limits. The yielding mechanism over the height of the structure is distributed uniformly as per the PBPD assumption (Fig. 7 b). Fig. 8 shows a comparison of entire columns for all frames. The leveling of Fig. 8 & 9 graphs have been carried out based on the leveling of Fig. 2(b,c & d). In the case of BRB configuration-I, ground columns are reaching just the ultimate condition. Also, the entire beams have reached their ultimate level. Few of the first and second columns are yielded while top outer bay columns show elastic behavior. Also, some of the first and second-floor columns reached the ultimate level. These observations can be observed in Fig. 7b. Meanwhile, all the BRBs have reached their ultimate capacity, which is expected as per the PBPD design assumption. Similarly, BRB configuration-II shows a uniform yield mechanism. The condition of the ground column is similar to BRB configuration-I. In this configuration, mid bays has higher stiffness than the outer bays so damaged has

attracted towards these bays. As a result, outer columns are within the elastic except second-floor columns. Also, the entire mid bays members (i.e. both column & beam) are reaching their yielding and ultimate level. As well, all the BRBs have reached their ultimate capacity. Fig. 9 shows the overall BRBs response comparison under static push over drift level of 4.0%.

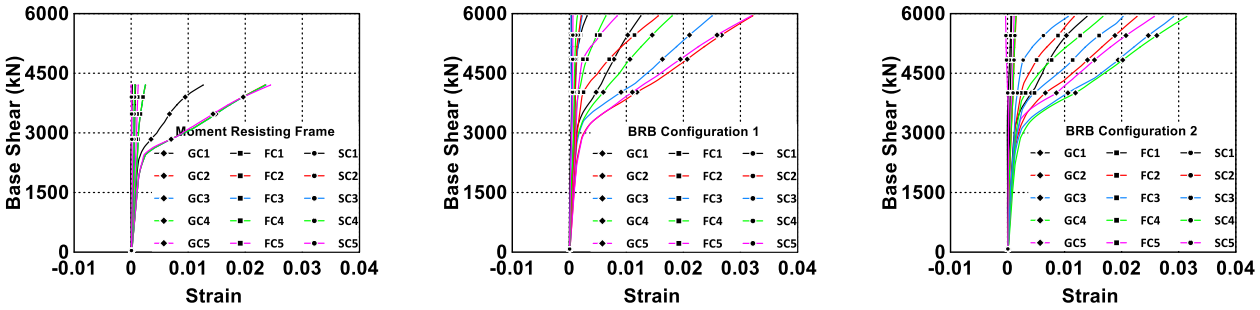

(a) (b) (c)

Fig. 8 – Comparison of column deformation (a) moment frame (b, c) BRB configuration-I & II

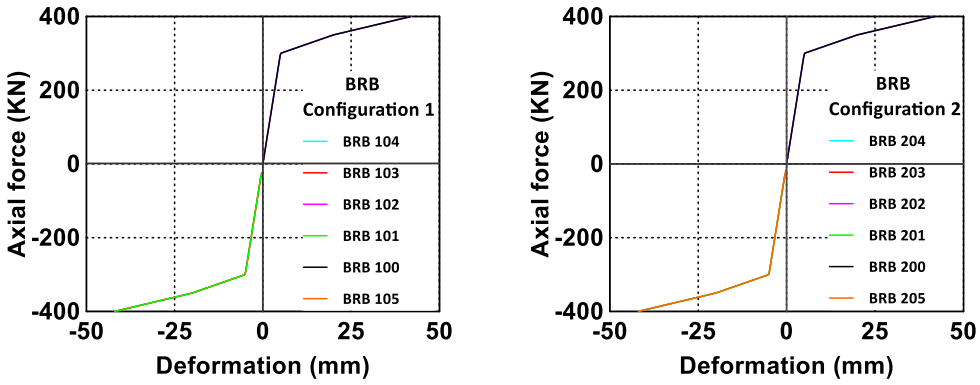

(a) (b)

Fig. 9 – Comparison of BRB deformation (a) configuration-I (b) configuration-II

5.2. Time history

Nonlinear time-history analyses are conducted on the study frames to evaluate their seismic response under the selected ground motions. The main parameters evaluated are (i) yield mechanism, (ii) drift response, (iii) hysteretic behavior, and (iv) response of BRBs.

Among the seven sets of ground motion, the MRF frame shows maximum deformation under the Kobe earthquake. It shows a drift value of 0.8% and 0.7% in the push and pull direction, and corresponding base shear values are 2948.1 kN and 2791.2 kN, respectively. Furthermore, the minimum MRF response is observed under the Kocaeli earthquake by bearing a drift level of 0.17% and 0.18% in the push and pull direction with corresponding base shear values of 834.4 kN and 759.4 kN, respectively. Similarly, BRBF-I & II frame also gets the maximum and minimum drift and base shear response under the same earthquake *(i.e., Kobe & Kocaeli)*. Table 4 summarizes the maximum base shear and drift response of all the frames for all ground motions. Overall Base shear vs. Drift response (*i.e., Hysteresis*) is shown in Fig. 10 and Fig. 11 shows the overall drift profile comparison of all study frames. These figures show how the BRBs controls the drift of structure without any changes in the structural section dimension. Also, there is no observation of instability in the structure due to buckling, fracture, etc. However, under the Chamoli and Kobe earthquakes, the MRF frame shows residual drift (Fig. 11), but this residual drift has been controlled in BRBFs due to its self-centering tendency. The BRBF-I and BRBF-II show different yield mechanism; however, overall performance like drift level, base shear are more or less the same; this can be observed from Table 4, Fig. 10 & 11.

Table 4 – Comparison of base shear vs drift response of all frames under selected seven Earthquakes

Name of Earthquake	Frame	Positive		Negative	
		Drift (%)	Base shear (kN)	Drift (%)	Base shear (kN)
Chamoli	*MRF*	0.68	2613.9	-0.62	-2435.6
	BRBF-I	0.19	1609.7	-0.32	-2769.4
	BRBF-II	0.19	1636.8	-0.33	-2784.2
Chi-Chi	*MRF*	0.69	2741.2	-0.67	-2836.1
	BRBF-I	0.19	1684.5	-0.33	-2683.6
	BRBF-II	0.18	1599.6	-0.33	-2635.4
El-Centro	*MRF*	0.62	2550.8	-0.61	-2497.5
	BRBF-I	0.31	2379.0	-0.36	-2818.0
	BRBF-II	0.32	2362.7	-0.35	-2767.9
Hector Mine	*MRF*	0.46	2080.9	-0.47	-2064.9
	BRBF-I	0.26	2210.2	-0.25	-2122.1
	BRBF-II	0.26	2173.8	-0.24	-2065.1
Imperial Valley	*MRF*	0.46	2083.1	-0.46	-2118.1
	BRBF-I	0.27	2193.5	-0.29	-2371.8
	BRBF-II	0.25	2085.0	-0.28	-2235.5
Kobe	*MRF*	0.80	2948.1	-0.70	-2791.2
	BRBF-I	0.36	2801.1	-0.41	-2887.4
	BRBF-II	0.35	2703.4	-0.40	-2792.8
Kocaeli	*MRF*	0.17	834.4	-0.18	-759.4
	BRBF-I	0.13	1168.2	-0.17	-1468.6
	BRBF-II	0.13	1172.0	-0.17	-1455.0

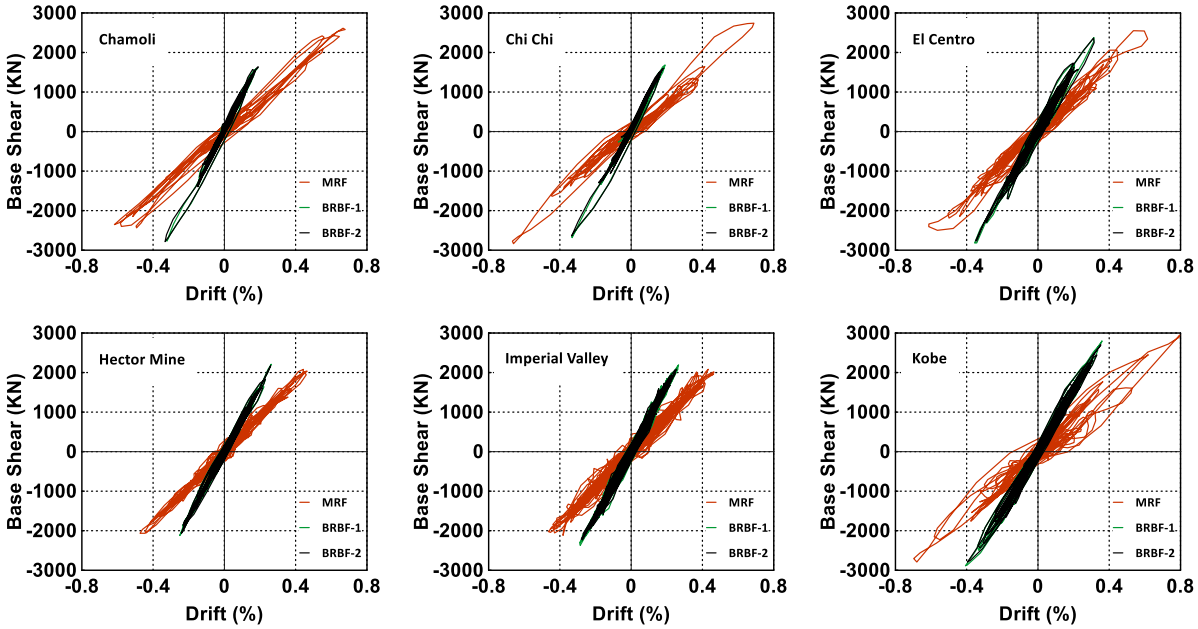

Fig. 10 – Base shear vs. Drift response of all study frame for all ground motions

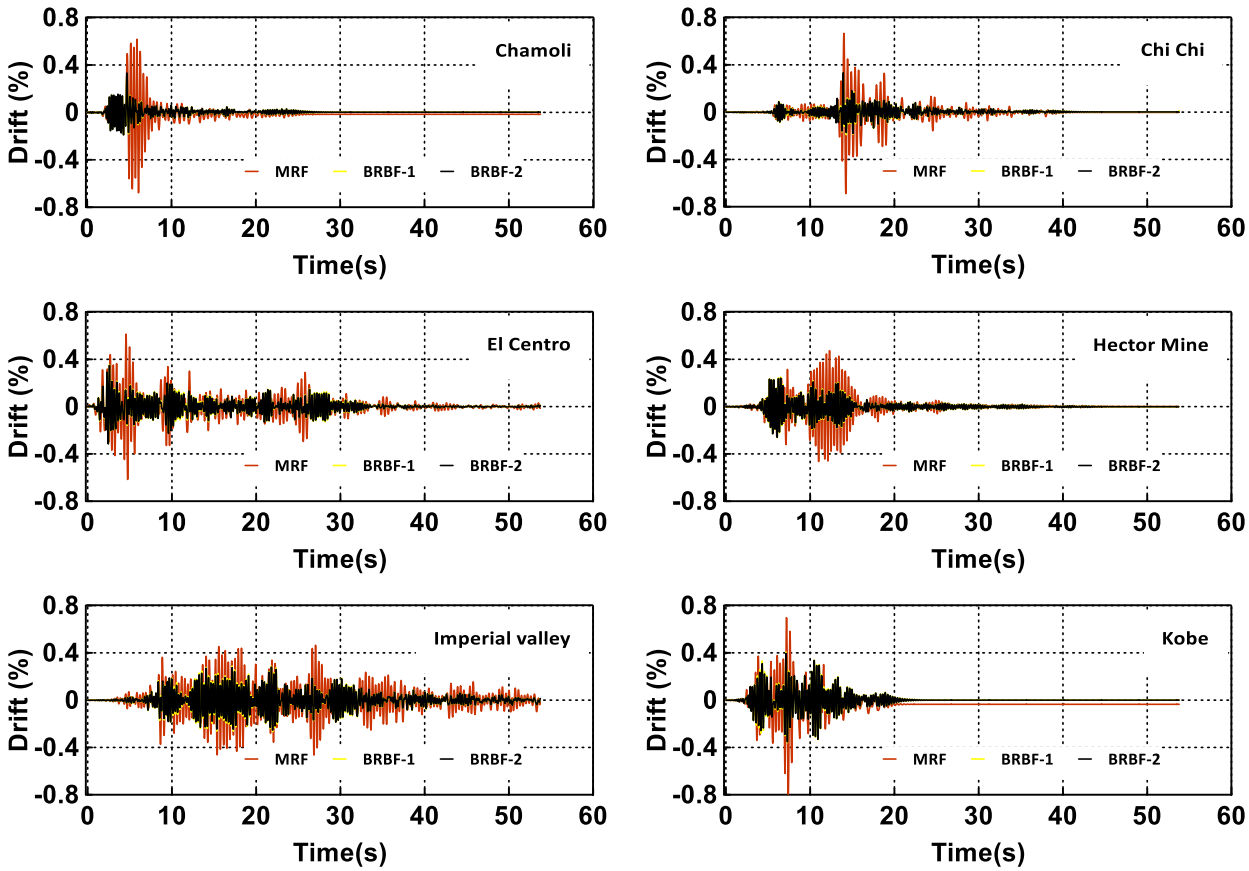

Fig. 11 –Drift response of all study frame

Table 5 summarised overall drift reduction due to BRBs. Incase of BRBF-I, the maximum and minimum drift reductions are observed as 52.94 % and 5.56%, respectively, which has been monitor under the Chamoli and Kocaeli earthquake. Similarly, for BRBF-II, the maximum and minimum reductions are observed as 52.17 % and 5.56 % under the Chi-Chi and Kocaeli earthquake. Fig. 12 shows the percentage of drift reduction due to BRBs as a bar chart.

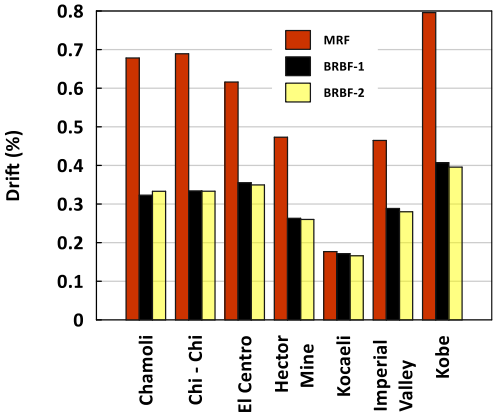

Fig. 12 –Comparison of drifts between the study frames.

Table 5 – Comparison of drift reduction due to BRBs

Name of Earthquake	Maximum Drift (%)			% of Drift Reduction	
	MRF	*BRBF-I*	*BRBF-II*	*BRBF-I*	*BRBF-II*
Chamoli	0.68	0.32	0.33	52.94	51.47
Chi -Chi	0.69	0.33	0.33	52.17	52.17
El-Centro	0.62	0.36	0.35	41.94	43.55
Hector Mine	0.47	0.26	0.26	44.98	44.68
Imperial Valley	0.46	0.29	0.28	36.96	39.13
Kobe	0.80	0.41	0.40	48.75	50.0
Kocaeli	0.18	0.17	0.17	5.56	5.56

BRBs are working effectively in the frame under extreme loading conditions. As a result, vibration control has improved significantly compared to MRF. Fig. 13 shows the response of the BRBs under all selected ground motions for all configurations. Different levels of deformations on BRBs are observed on different

floor levels, which happen due to different demands on each floor under lateral loading. Out of the seven ground motion, six ground motion has a high impact, which causes the deformation of BRBs within the permissible non-linear level. In the case of the Kocaeli earthquake, BRBs in both the frames are just yielded, without any extensive damage. In the El-Centro and Kobe earthquakes, extensive deformation has been observed in BRBs. Under these two earthquakes, BRBs are dissipating more energy.

Meanwhile, less damage has been observed in the remaining part of the frame, which indicates that the BRBs are activated effectively and able to deform as per the design target. In the BRBFs systems, overall energy dissipation capacity, ductility, and lateral load-carrying capacity are significantly improved due to the major contribution of BRBs. This conclusion is made based on pushover analysis as well as time history analysis (Fig. 7, 9, 10, 12, 13).

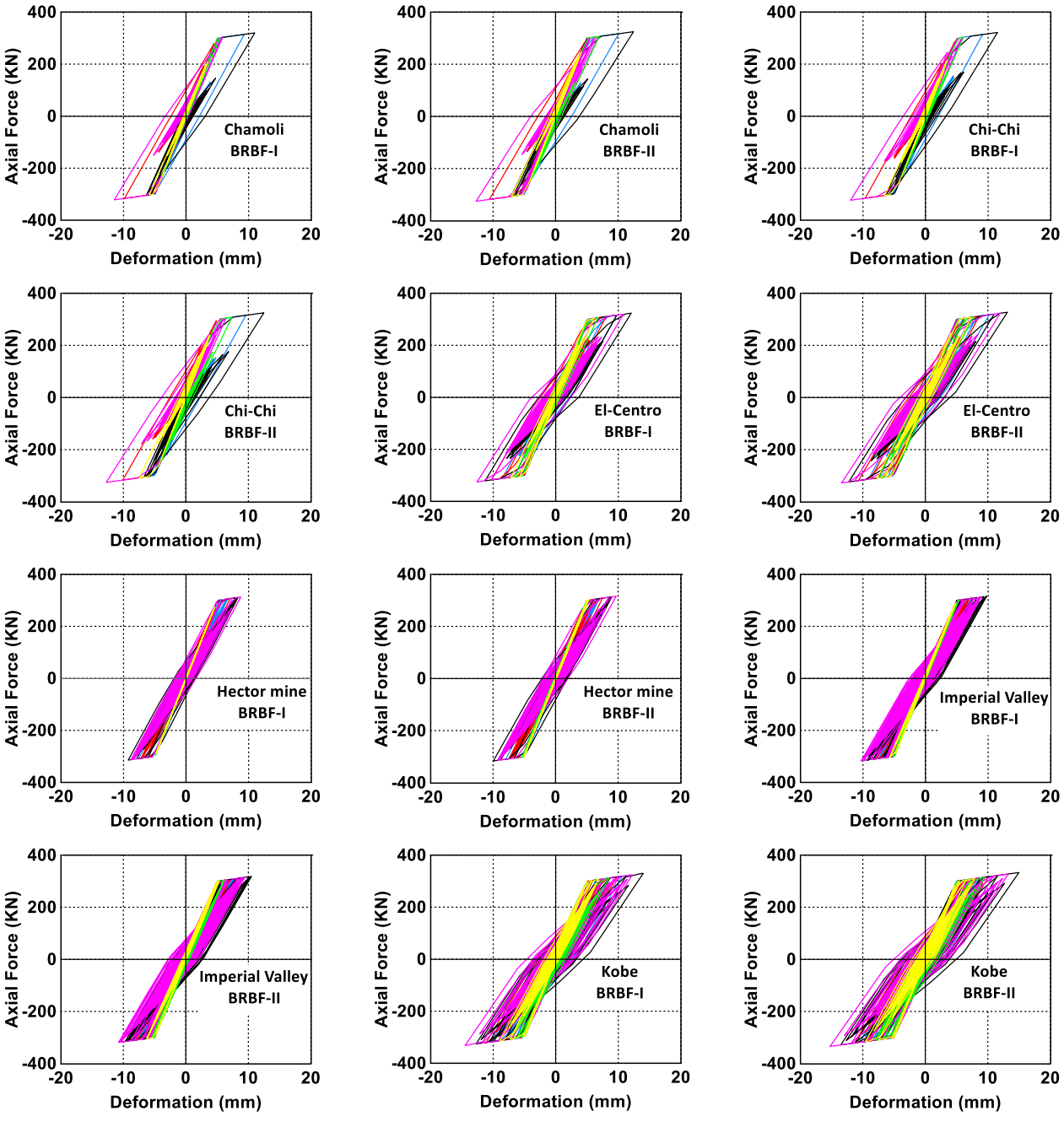

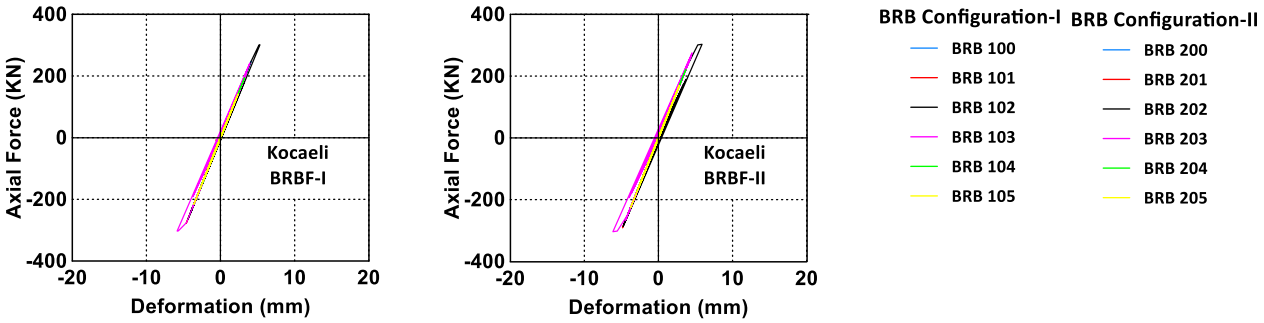

Fig. 13 – BRBs responses under various Earthquake loading

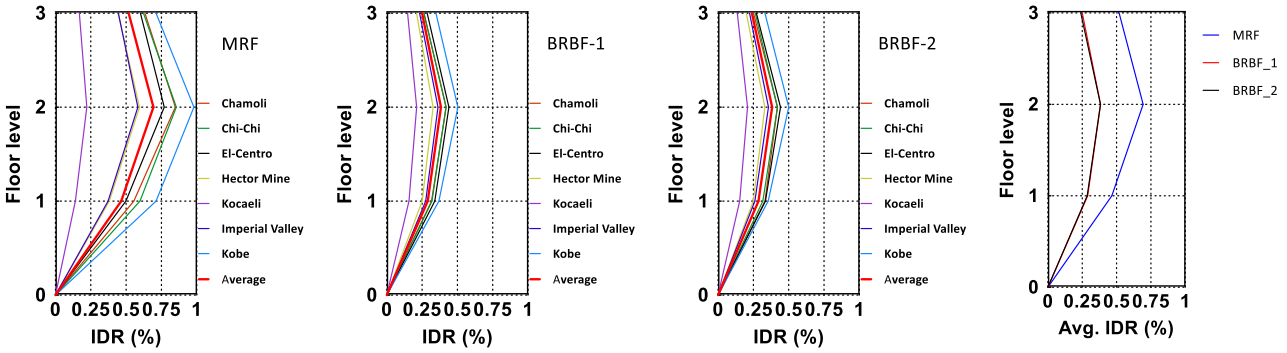

(a) (b) (c) (d)

Fig. 14 – Comparison of inter-story drift (IDR) (a) moment frame (b) BRBF-I (c) BRBF-II and (d) average IDR of all frame

Fig. 14 shows the comparison of peak inter-story drift ratio (IDR) response of the frames under the selected ground motions. The peak values of IDR are noted at the second-floor levels with lesser inter-story drift at the upper story. The maximum value of IDR for the MRF frame is noted as 0.98% in Kobe ground motion. The mean value of peak IDRs for seven ground motions is found to be 0.69% for the MRF frame. For the BRBF-I, the maximum IDR value is noted as 0.51% in Kobe ground motion, and the mean IDR value is found to be 0.38%, indicating a reduction of about 50.0% in the peak IDR response due to the proposed BRB configuration-I. In the case of BRBF-II, a significant reduction in the peak value of IDR is noted, i.e., from 0.98% to 0.50%. The mean values of IDR for the BRBF-II is found to be 0.37%. A comparison of average IDR values is shown in Fig. 14d. The BRBFs system controls the drift, and IDR significantly compared to MRF due to the resiliency of BRBs (Fig. 11, 12 & 14; Tables 4 & 5).

5.3. Results and discussion

Compared to the MRF frame, the BRBFs frame shows better performance in terms of load-carrying capacity, drift, vibration, and distribution of yielding along with the height of the frame. However, BRBF-I & II are not much significant in all directions except in the yielding mechanism. In the case of BRBF-II, yielding has been concentrated in the middle bays due to high force attraction. On the other hand, BRBF-I show yielding in mid bays as well as outer bays mainly on top floors. If we look only on yield mechanism, BRBF-I is preferable due to its distributed yielding pattern. Otherwise, the overall performance point of view both configurations are vise versa.

6. Conclusion

This study has been carried out to investigate the performance of different BRB configurations along with the moment frame, which is designed using Performance-based plastic design (PBPD). Based on this study, the following points have been drawn as a conclusion:

a. The Performance-based plastic design is a strong design methodology, which could provide an optimum section based on the preferable yield mechanism.

b. The failure mechanism of all study frames is the same as per the design assumption.

c. BRBs could influence the yield mechanism of the frame; however, overall performance is more or less the same.

d. Energy dissipation capacity, ductility, and lateral load-carrying capacity of the BRBF systems are significantly higher than the MRF system.

e. The residual drift of the frame could be control by BRBs due to its self-centering behavior.

f. The fiber section could consider the non-linear deformation of the frame members, which is more realistic than the lumped mass plastic hinge models.

g. *OpenSees* has the capability of modeling all kinds of non-linearity using its vast material library. In the current model, the non-linear behavior of BRBs has been captured.

7. References

[1] Sahoo DR, Chao SH (2015): Stiffness-based design for mitigation of residual displacements of buckling-restrained braced frames. *Journal of Structural Engineering*, **141** (9), 04014229: 1-13.

[2] Erochko J, Christopoulos C, Tremblay R, Choi H (2011): Residual drift response of SMRFs and BRB frames in steel buildings designed according to ASCE 7-05. *Journal of Structural Engineering*, **137** (5), 589-599.

[3] ASCE 7-16 (2016: *Minimum design loads for buildings and other structures*. American Society of Civil Engineers.

[4] Goel SC, Chao SH (2008): *Performance-based plastic design: Earthquake-resistant steel structures*. International code council.

[5] Housner GW (1956): Limit design of structures to resist earthquakes. *1st World Conference on Earthquake Engineering*, Berkeley, USA.

[6] Goel SC, Liao W, Bayat MR, Chao SH (2010): Performance-based plastic design (PBPD) method for earthquake-resistant structures : An overview. *Structural Design of Tall and Special Buildings*, **137** (19), 115-137.

[7] IS:1893-I (2016): *Criteria for earthquake resistant design of structures: General provisions and buildings*. New Delhi: Bureau of Indian Standards.

[8] McKenna FT, Fenves G, Scott M, Jeremic B (2000): Open system for earthquake engineering (OpenSees). *University of California*, Berkeley USA.

